Available online at www.sciencedirect.com

ScienceDirect

journal homepage: www.elsevier.com/locate/he

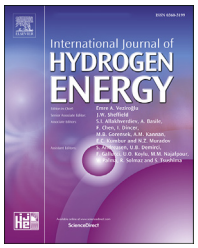

Experimental simulations of hydrogen migration through potential storage rocks

Bettina Strauch[*], *Peter Pilz*, *Johannes Hierold*, *Martin Zimmer*

GFZ German Research Centre for Geosciences, Telegrafenberg, 14473 Potsdam, Germany

HIGHLIGHTS

- An experimental setup to investigate hydrogen diffusion in rock samples was designed.
- Hydrogen diffusion coefficients and breakthrough times were successful determined.
- First results for sandstone, rock salt, claystone samples were generated.
- Site-specific studies of hydrogen migration in geomaterial for storage is possible.

ARTICLE INFO

Article history:
Received 22 December 2022
Received in revised form
10 February 2023
Accepted 10 March 2023
Available online 7 April 2023

Keywords:
Experimental simulation
Hydrogen breakthrough time
Hydrogen diffusion coefficient
Opalinus clay
Werra rock salt
Bentheimer sandstone

ABSTRACT

In the framework of future decarbonization of the energy industry, the safe and effective storage of hydrogen is an important approach to add to a climate-friendly energy system. Until the development of sufficiently large electrical storage systems, the storage of hydrogen in the order of GWh to TWh is envisaged in salt caverns or porous geological formations with a gas-tight covering of salt or claystone. In order to calculate gas losses from these H_2 storage facilities, the H_2 diffusivity of the storage and cap rocks must be known. To determine the hydrogen diffusion rates in these rocks, an experimental set-up was designed, constructed and tested. The set-up comprises two gas chambers, separated by the rock sample under investigation with an exposed area of approximately 7 cm^2. The driving force for gas migration through the rock sample from the hydrogen-containing feed gas chamber to the hydrogen-free permeate chamber is the chemical potential (concentration) gradient. With respect to hydrogen migration behaviour, hydrogen breakthrough times and hydrogen diffusion coefficients were determined for dry and wet Bentheimer sandstone, Werra rock salt and Opalinus clay samples. Breakthrough times varied between less than 1 h and 843 h. Based on concentration changes at the permeate side, hydrogen diffusion coefficients were derived ranging from 10^{-9} to 10^{-8} m^2/s. The differences between the materials and the effect that wetted or water-saturated samples have higher hydrogen retention due to closed pores and microcracks were clearly shown. The experimental set-up proves to be a suitable approach to determine site-specific rock characteristics such as hydrogen diffusion coefficients and breakthrough times for natural geomaterials.

* *Corresponding author.*
E-mail address: betti@gfz-potsdam.de (B. Strauch).

https://doi.org/10.1016/j.ijhydene.2023.03.115

Introduction

Hydrogen is one of the most promising clean energy sources of modern times [e.g. 1,2]. As an environmental-friendly fuel, it plays a major role in reducing greenhouse gas emission and ease climate changes [3]. In national and international hydrogen strategies the topic of geological hydrogen storage plays an important role in the intended use of seasonal excess capacities of renewable electricity [e.g. 4,5]. Common renewable energy sources, such as wind, solar and hydro energy are often subject of seasonal and daily fluctuations. The discrepancy between demand and supply could be bridged by converting surplus energy into hydrogen and storing it underground [6]. In salt caverns and porous rock formations (aquifers and depleted natural gas fields) the storage of hydrogen energy is predicted in the order of megawatts to terawatts [7]. To assure the long-term safety and economic viability of such storage systems, effective tools for the site evaluation are needed [8]. As there is limited experience with geological hydrogen storage [9], extensive research is currently conducted to address a variety of issues to ensure the safe and effective hydrogen storage [10–16]. This includes studying the interaction of hydrogen with minerals in different geological formations (coal, sandstone, salt, carbonate), wettability, microbial and geochemical activities, the influence of pressure, temperature and organic matter [e.g. 17–21]. Furthermore, the permeation or diffusion of hydrogen through reservoirs and cap rocks, the dissolution in the pore fluids and the chemical reactions of rocks and fluid components are in the focus of modeling studies [22–25].

Since rocks and pore fluids have individual properties depending on the site, location-specific studies are needed for a reliable prediction of hydrogen storage performance, hydrogen flow behaviour and fluid-rock interactions. In this context, experimental simulations of hydrogen diffusion through natural rocks provide the necessary real data for successful model verification and thus, for a profitability and safe long-term geological hydrogen storage.

Gas diffusion coefficients have already been experimentally determined and validated for various rock types using air or common gases such as nitrogen, oxygen, methane and carbon dioxide, helium, light hydrocarbons and carbon monoxide [15,26–28]. Hydrogen diffusion in natural rock samples, however, has not been well studied.

In contrast, since the first observation by Graham in 1866 [29], that hydrogen diffuses through platinum, the phenomena of hydrogen diffusion through metals have been subject of many investigations [30]. Gas-based permeation experiments were later used by Stross and Tompkins [31] or Johnson [32] to obtain diffusion coefficients of hydrogen in iron material as a function of temperature. For hydrogen diffusion in iron, values between 3×10^{-5} cm^2/s and 7.5×10^{-5} cm^2/s are given by Oriani [33] and Addach et al. [34], respectively.

Data of hydrogen diffusion coefficients in pure water can also be found in literature. They range from 3.9 to 6.1×10^{-9} m^2/s [35–39].

A hydrogen diffusion coefficient in saturated brine was reported by AbuAisha and Billiotte [40] to be 4.6×10^{-9} m^2/s.

Reports on hydrogen diffusion coefficients in air are in the range from 0.756 to 1.604×10^{-4} m^2/s [39,41].

Hydrogen diffusion coefficients for natural rock samples are sparse in the literature. Data for water-saturated clayed host rock and Boom clay are given as 3×10^{-11} m^2/s and 5.1×10^{-10} m^2/s, respectively [38,42]. For salt grit, diffusion coefficients between 1 x 10^{-7} m^2/s and 6×10^{-12} m^2/s, are given in Müller-Lyda [43] depending on salt type, degree of compaction and moisture content.

The work presented here was initiated to improve the data availability on hydrogen diffusion coefficients through natural rock samples. For this purpose, a measurement concept was developed, using two gas chambers, separated by the rock sample under investigation. With the help of an internal amperometric hydrogen sensor, long-term experiments could be carried out without gas sampling for external analysis. The background to this is, that any form of gas extraction for external gas measurements creates a pressure gradient that influences the hydrogen diffusion behaviour. The migration of gas through solid rock bodies is driven by the gradient of the chemical potential or, simplified controlled by a concentration or pressure gradient. Without force, the permeate moves towards lower concentration or lower partial pressure [e.g. 44]. In the feed chamber, the hydrogen concentration is higher than in the permeate side. Therefore, the hydrogen molecules are adsorbed on the surface of the separating rock sample, then the hydrogen is absorbed by the material and diffuses through pores and molecular interstices of the sample. When the hydrogen molecules reach the other side of the sample, the hydrogen is released by desorption and enters the permeate gas chamber.

The main objectives of the study presented here are (i) to verify the functionality and practicability of the experimental setup for the investigation of site-specific rock samples in form of core material and (ii) to provide a first characterization of hydrogen diffusion through different rock types in context of hydrogen storage.

Methods

Experimental setup

The diffusion cell was designed and constructed using standard components (flanges, hoses, fitting elements, gaskets in accordance with the CF standard ISO3669 from VACOM Company). Two cylindric tee tube connectors were used to create an inlet feed and a permeate chamber. CF seals, made of oxygen-free, high-purity copper were used for a maximum of tightness. Two-way valves (FITOK Company) were used for the gas inlet and outlet ports on the feed side and for a single outlet port on the permeate side. On the permeate side, the second tube opening was closed by a flange with an electrical feed through to install a modern solid-state hydrogen sensor (H_2 SS micro, EUROGAS Company) in the permeate cell. It has a measurement range of 0–20,000 ppm hydrogen. The measurement is based on the principle of electrochemical gas detection. When hydrogen hits the electrolyte of the measurement electrode, it forms two protons ($2H^+$) and two

electrons. The number of electrons corresponds to the concentration of hydrogen and is detected as a current. Similarly, the protons move to the counter electrode and form water with ambient oxygen. The isolated reference electrode maintains the base potential and stabilizes the sensor output.

The hydrogen sensor was mounted to a SS PCB transmitter (EUROGAS Company) and data connection was realized via a pin port to a data logger (Meier NT Company) for online data monitoring and read out. Feed and permeate cells cover a volume of 0.2 L, respectively. They are connected by the sample-carrying through flange (Fig. 1). Here, the sample is embedded with epoxy resin (ROTH Company). The experiments were all performed at ambient pressure and temperature conditions at both, feed and permeate cell. So, potential contamination caused by pressure-induced leakage could be prevented.

Sample material and preparation

For the investigation of hydrogen diffusion, rock types were chosen, that are potentially in contact with hydrogen during underground storage. Typically, salt caverns and groundwater-bearing sandstones with caprock are considered as intermediate storage sites for hydrogen. Therefore, core pieces of Werra rock salt, Bentheimer sandstone and Opalinus claystone were selected for the experiments. Note, that these are pristine rocks with no previous contact to hydrogen.

The Bentheimer sandstone samples were obtained from the archive of RWTH Aachen University and are homogenous core material of 30 mm diameter. The samples have a porosity of 23.7% (pers. com. RWTH Aachen), permeabilities are reported between 0.52 and 3.02 Darcy ($5.13–29.8 \times 10^{-13}$ m^2) by Peksa et al. [45]. Details on petrographic characteristics can be found in the literature, e.g. in Dubellar [46].

The Werra rock salt samples originate from the Middle Werra rock salt of the Zechstein formation (z1NAb). The cores were dry-drilled from an underground gallery of the Werra-Fulda mining district (Hessian, Germany) during sampling campaigns in 2017 [47]. For core samples of this location, a porosity of 0.5% was determined. Permeability data for rock salt in a range from 10^{-20} to 10^{-22} m^2 were published by Stormont [48].

The Opalinus clay was recovered in 2021 from the Mont Terri Rock Laboratory, Switzerland during a drilling campaign (core BHS-1). According to Al Reda et al. [49] and Bock [50]; Opalinus clay has a porosity of 9.6% to almost to 13%, respectively. Permeability data in a range from 6.9×10^{-21} to 2.3×10^{-19} m^2 are reported by Al Reda et al. [49] and Jacops et al. [51].

The sample material of Werra rock salt and Opalinus clay were stored air-tight in vacuumed aluminium bags to avoid contact and contamination with ambient air.

The cores were sliced into pieces of a certain length. For the work presented here, 10 mm thick discs were prepared. Tests with longer plugs are equally possible using self-manufactured through flanges or cylindrical tube connectors in which the plug will be fixed with epoxy resin. Having 30 mm diameter, the exposed surface area of the sample section always covers 7 cm^2.

Before mounting the sample discs to the through flange, the surrounding mantle area was coated with viscous epoxy resin and allowed to dry for 24 h. The discs were then placed into the inner flange and fixed in place using fitted silicone forms. The upper part of the core was then bonded to the flange by carefully pouring liquid epoxy into the gap between core and flange.

After the drying period, the flange-core-silicone piece was turned upside down, the silicone form was removed and the remaining gap was filled with epoxy resin and left for another 24 h drying.

Now, the plug was ready to be used. The flange was placed as intermediate piece between the feed and permeate chamber (Fig. 1).

For experiments using water- or brine-saturated Bentheimer sandstone samples, the prepared core-flange pieces were vacuum-dried and placed in a beaker in an exsiccator. The exsiccator with sample was evacuated to empty the samples pore space before the sample was then exposed to inward-poured deionized water or brine that filled the beaker. The sample was then stored in the liquid-filled beaker until it was placed into the diffusion apparatus between feed and permeate chamber.

Experimental run

The feed chamber was purged with a gas mixture of 2 vol% hydrogen in synthetic air (AIRLIQUIDE Company) at ambient pressure for 5 min, through the feed gas inlet and outlet port (Fig. 1b). The permeate chamber contained ambient air and was equipped with a hydrogen sensor for the continuous measurement of hydrogen concentration in the permeate gas, for the whole experimental time period.

The complete data sets (measured, uncorrected and corrected hydrogen concentrations at the permeate chamber,

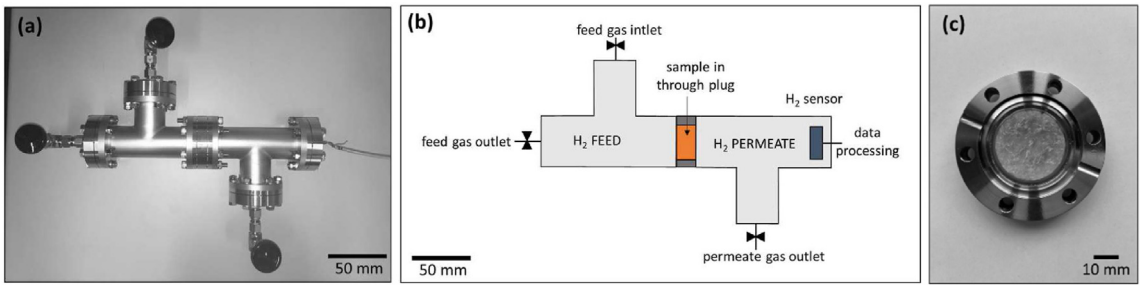

Fig. 1 – (a) Picture of experimental set-up; (b) schematic drawing of diffusion cell; (c) through flange with embedded Werra rock salt sample.

temperatures) are published in the corresponding data publication Strauch et al. [52].

Since there is no pressure gradient, the driving force for gas movement through the sample plug is solely the concentration gradient of hydrogen between the feed and the permeate chamber. The hydrogen breakthrough is marked by the first detection of hydrogen at the hydrogen sensor. The diffusion rates are determined from the subsequent increase in hydrogen concentration in the permeate chamber.

Various tests were performed prior to routine measurements to ensure the tightness and technical correctness of the diffusion cell set-up.

The leak tightness of the epoxy resin, embedding the sample plug, was tested to assure that hydrogen migration occurs through the sample but not through the surrounding bedding material. For the test, a metal plug of similar size as the sample plugs (30 mm diameter and 10 mm thickness) was embedded in epoxy resin and a trial run similarly to the real tests was performed. Within three month run time no hydrogen was detected at the permeate side, confirming the quality of epoxy resin in terms of gas tightness for experiments with low hydrogen concentration gradients at atmospheric pressure conditions [53].

The tightness of the feed gas chamber was ensured by external analyses. During initial tests, with gas tight plugs, the gas concentration at the feed chamber was checked by extracting about 2 cm^3 of gas sample through a gas tight septum with a syringe. A gas mass spectrometer (PFEIFFER Company) was used for analyses. The results showed no decrease in hydrogen concentration in the feed cell, so we concluded, that the feed compartment was tight.

To test the tightness of the permeate side, direct measurements were made with the micro hydrogen sensor. We observed decreasing hydrogen concentrations with time. Therefore, detailed measurements were performed using a "single cell set-up". In this way, we were able to reduce the origin of hydrogen-loss to two possibilities. Either the sensor itself consumes a certain amount of hydrogen during permanent analyses, or the electrical feed-through port of the sensor is not leak-tight to hydrogen. Regardless of the sink origin, we were able to establish a hydrogen-loss correction equation for the correction of the results of diffusion experiments.

Determination of hydrogen-loss correction equation

The hydrogen-loss rate was determined in repeated experimental runs, with a "single cell set-up", which a separate, closed permeate cell including the micro hydrogen sensor. The cell was purged with the check gas containing 2% hydrogen in synthetic air. The decrease of hydrogen concentration with time was monitored (Fig. 2) and the values from 10,000 ppm downwards were used to calculate the hydrogen-loss. Higher values were excluded because the maximal concentration during diffusion experiments will be 10,000 ppm on the feed side (20,000 ppm is the initial concentration at the feed side, after diffusion and reaching equilibrium between the two reservoirs, the concentration should be 10,000 ppm hydrogen at each side).

The concentration decrease was non-linear, with the highest hydrogen-loss rate at the beginning of the run and the lowest hydrogen-loss rate at the end of the experiment (Fig. 2a). Based on that, a correlation between hydrogen concentration in the chamber and hydrogen-loss rate can be derived (Fig. 2b). The difference between the nominal value and the real value is the hydrogen-loss rate per hour. The lower the concentration in the chamber, the lower the hourly loss, e.g. having about 8000 ppm hydrogen in the chamber, the loss is roughly 300 ppm/h, at concentration of 5000 ppm in the permeate chamber, the loss is only 100 ppm/h. The correlation is shown in Fig. 2b. There are highly scattering data points at hydrogen concentrations above 8000 ppm. Therefore, only values below 8000 ppm were used for the calculation of the best fit equation.

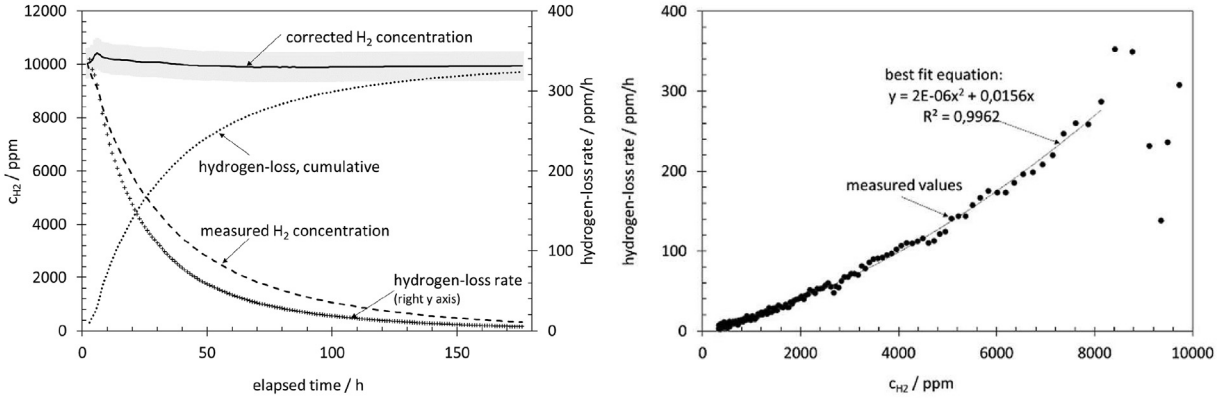

Fig. 2 – (a) The diagram shows the decrease of measured hydrogen concentration and the corresponding increase in cumulative hydrogen loss (primary y-axis) in the single cell, within one week. It also shows the corrected hydrogen concentrations with a 5% error range. The hydrogen-loss rate in ppm per hour (thin crossed marks) corresponds to the secondary y-axis. (b) The diagram shows the hydrogen-loss rate as a function of the hydrogen concentration in the single cell.

The following best fit equation was derived by repeated tests on the single cell set-up and subsequently used for the hydrogen-loss correction of the measured hydrogen concentration on the permeate side in the course of a diffusion experiment.

$$Q = 2 \times 10^{-6} (c_{H_2})^2 + 0.0156\, c_{H_2} \qquad \left[\frac{ppm \times 200\ cm^3}{h}\right]$$

The hydrogen-loss rate Q was calculated in ppm for the permeate cell volume of 200 cm^3 and time intervals of 1 h. The conversion into conventionally used units of [mbar x liter/sec] was not considered suitable for the application and set-up used here.

As can be seen in Fig. 2a, the corrected values fit well with the expected hydrogen concentration of 10,000 ppm in the chamber. However, at the beginning of the experiment, when the hydrogen concentration is highest and the hydrogen-loss is also highest, the calculated corrected values are higher than the expected true value (above 10,000 ppm). Therefore, an error bar of 5% was added to the calculated data.

Determination of the corrected hydrogen concentration at the permeate side

Fig. 3 shows the result of an experiment with water-saturated sandstone. The measured hydrogen concentrations (dashed line) increased to values of about 1200 ppm after 215 h. From then on, the concentrations remained relatively levelled with slightly decreasing trend in hydrogen concentrations over time. The experiment was terminated after 350 h.

The calculated hydrogen-loss rate raised to values up to 25 ppm per hour at times when maximum hydrogen concentrations were measured (at about 200 h elapsed time). At constant hydrogen concentrations at the permeate cell, the hydrogen-loss rate remained relatively leveled between 20 and 25 ppm hydrogen-loss per hour. The subsequent calculation of corrected hydrogen concentrations revealed, that the concentration of hydrogen on the permeate side was actually still increasing. This indicates, that the diffusion process through the rock sample was still ongoing when the experiment was stopped. For equilibrium between feed and permeate chambers, the hydrogen concentration should have reached values of about 10,000 ppm. However, the observation time was sufficient for the calculation of diffusion coefficients. Only a linear increasing concentration range was required for the calculation.

Determination of the breakthrough time

The breakthrough time, or lag time, is in the literature often defined as intercept of abscissa by the extension of the linear part of the graph of hydrogen concentration versus elapsed time [e.g. 54,55]. However, In case of a rather shallow increase in permeate concentration, the graphical determination of lag times results in too low or even negative values. Therefore, in this study we state the breakthrough time as the time interval between the start of test gas purging of the feed chamber and the first detection of hydrogen at the hydrogen sensor in the permeate chamber. Depending on the sample material and water saturation, it ranged from minutes to months (Table 1). The complete data set is available in the corresponding data publication of Strauch et al. [52].

Determination of diffusion coefficient

In contrast to homogeneous materials such as metals or polymers, the texture and microstructure of natural rock samples are highly complex. For instance sedimentary rocks consist of mineral grains or mineral aggregates, a mineral binder and pore space. The latter can be either wetted, or filled

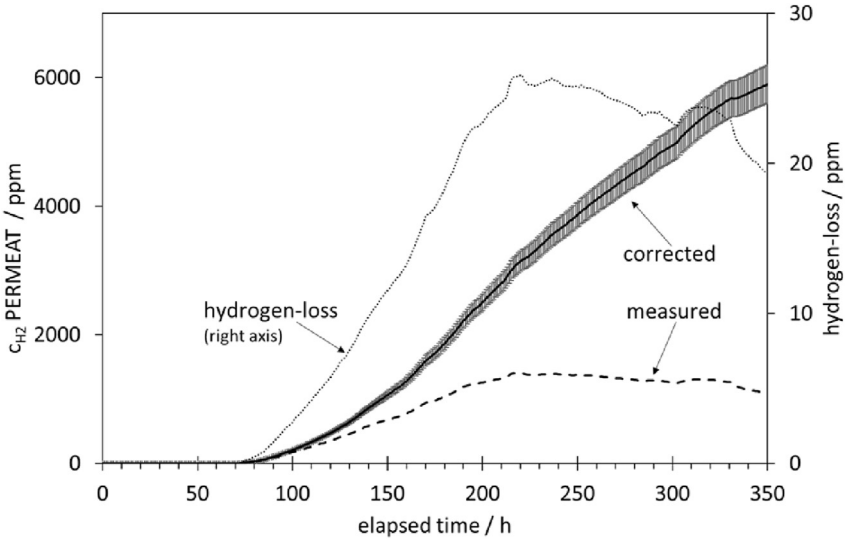

Fig. 3 – Diagram showing the progressions of hydrogen concentration at the permeate side during an experiment testing a water-saturated sandstone plug. The dashed curve refers to the measured values, the black line indicates the corrected data, based on the hydrogen-loss rate (dotted line, referring to the secondary y axis). The 5% error bars are implemented on the corrected graph.

Table 1 – Summary of experimental results, showing calculated hydrogen diffusion coefficients, breakthrough times and experimental run time for different natural rock samples. The internal name is stated for tracing data sets of the experiments in the accompanied data publication Strauch et al. [52].

Experiment #	internal name	sample material	diffusion coefficient [m^2/s]	breakthrough time [h]	run time [h]
1	H2R2-21	Bentheimer sandstone	2.1E-09	2	106
2	H2R2-18	Bentheimer sandstone, water saturated	1.6E-09	73	355
3	H2R2-07	Werra rock salt	1.3E-08	1	82
4	H2R2-09	Werra rock salt, wetted	1.4E-09	843	2024
5	H2R2-24	Opalinus clay	1.8E-09	2	788
6	H2R2-26	Opalinus clay, wetted	1.2E-09	2	477

with gas, fluids or a mixtures of both. The molecular diffusion of gases through rock samples is therefore always a combination of diffusion in gases, liquids and solids. Consequently, with increasing porosity and permeability of the rocks, hydrogen diffusion through the solid becomes less important. This type of diffusion is usually described by an effective diffusion coefficient (D_e). If the rocks also contain clay minerals, sorption effects on the clay mineral surfaces can influence molecular diffusion. In this case, D_e is extended by the sorption effect to the apparent diffusion coefficient (D_a).

Since the distinction between diffusion types is not considered for the rocks examined here, and simply the whole-rock samples were investigated, the unspecified term "hydrogen diffusion coefficient" is used. This term comprises the hydrogen diffusion through the whole-rock sample, including diffusion through minerals, gas and liquid within pore spaces or micro fractures, as well as all kind of side effects.

For the determination of the hydrogen diffusion coefficent, the corrected hydrogen concentrations c_{H2} at the permeat side were used in a time span, where the concentration increase per time remained relatively constant. As shown in Fig. 4, the hydrogen concentration c_{H2} increased rapidly after hydrogen breakthrough, as shown by the steep increase in the differences of hydrogen concentrations Δc_{H2} . After about 180 h, the Δc_{H2} remained at a high level with values up to 40 ppm. Here, the temporal range between 160 and 215 h of elapsed time was chosen for the calculation of the diffusion coefficent. Although the Δc_{H2} values scatter strongly, the range marks the area in which, overall, neither a further increase nor a incipient decrease of Δc_{H2} occurs.

The equation of Geiker et al. [56] was applied for the calculation of the diffusion coefficent D in m^2/s. The volume of the permeate cell (V), the area of the exposed sample (A) and the time difference between two measurements (Δt) are similar at 0.0002 m^3, 0.0007 m^2 and 3600 s, respectively for all experiments. The incremental differences between two hydrogen concentrations ΔQ, were calculated from the proximate values, as well as the gradient between the hydrogen concentration at the feed chamber (c_1) and the hydrogen concentration at the permeate side (c_2). The length of the sample (L) was 0.01 m.

$$D = \frac{V \times \Delta Q}{A \times \Delta t} \times \frac{L}{(c_1 - c_2)}$$

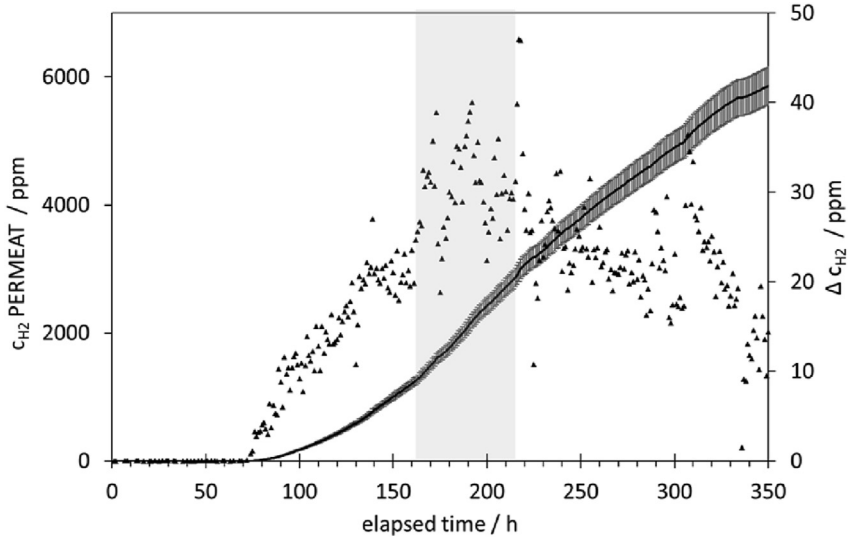

Fig. 4 – Diagram shows the corrected hydrogen concentrations c_{H2} on the permeate side (primary y-axis) and the concentration differences between two adjacent measurements Δc_{H2} (secondary y-axis). Shaded in grey is the area, where the increase in hydrogen concentration between two measurements is fairly constant (with no decreasing or increasing tendency). Data within that time range were used for the calculation of the hydrogen diffusion coefficient.

For the determination of the diffusion coefficient, a time span had to be chosen in which the hydrogen concentration on the permeate side is constantly increasing, indicating equilibrium conditions. This does not mean equilibrium between the reservoirs, but rather a steady-state diffusion of hydrogen through the sample.

Since the experimental set-up did not allow for constant hydrogen concentrations on the feed side, the feed concentration had to be constantly adjusted for the calculation. We assumed, that the corrected concentration detected at the feed side was the concentration by which the permeate concentration had to be reduced. This means, that as the concentration at the permeate side increased, the hydrogen concentration on the feed side decreased by the same amount (Fig. 5). Therefore, the concentration gradient between the feed and permeate side decreased in the course of the experiment as soon as hydrogen entered the permeate chamber.

The reproducibility of results is in the range of ±2%. This is valid for repeated diffusion experiment with the identical sample. When analyzing different core samples of similar rock material, the resulting diffusion coefficients remain in the same order of magnitude. The variations are likely the result of naturally occurring differences in the rock matrix, such as micro fissures or inhomogeneous pore filling.

Results and discussion

The results of diffusion experiments with dry and wet Bentheimer sandstone, Werra rock salt and Opalinus clay are presented here. Note, the term “dry” refers to the original conditions of the rock samples. We did not perform additional drying of sample material. Fig. 6 shows the typical course of the measured and corrected hydrogen concentration on the permeate side. The hydrogen concentrations are shown in hourly intervals. In addition, ΔQ values are shown at the secondary y-axis indicating the changes in hydrogen concentrations between two adjacent values.

Overall, samples used here were permeable to hydrogen, but had some different characteristics in terms of breakthrough times and hydrogen diffusion progression. The highest diffusivity was found for the dry Bentheimer sandstone (Fig. 6a) and the dry Werra rock salt (Fig. 6c). By far the lowest hydrogen diffusion was detected for the wetted Werra rock salt sample (Fig. 6d).

Measurements on dry sandstone, salt and clay material

Measurements on the dry Bentheimer sandstone resulted in a hydrogen breakthrough time of about 1 h. As can be seen in Fig. 6a, within the first 3 h after hydrogen breakthrough, the hydrogen concentration at the permeate side increased strongly between two measurements to values above 250 ppm per hour (ΔQ). After 15 h, the maximum measured hydrogen concentration was reached with approximately 3000 ppm. The measured concentrations slowly decrease to 2000 ppm after 70 h run time. The concentration changes ΔQ showed scattering around 25 ppm/h, and the values remained below 50 ppm/h. The correction curve shows, that hydrogen concentrations in the permeate chamber were actually still increasing. After 70 h run time, the calculated concentration is about 5000 ppm and equilibrium in hydrogen concentration between feed an permeate chambers was not achieved. The time span between 20 and 70 h was used to calculate the diffusion coefficient.

A similar observation was made for the hydrogen diffusion through dry Werra rock salt (Fig. 6c). Again, the breakthrough time was fast and hydrogen was detected within the first hour after the start of the experiment. The changes in hydrogen concentration ΔQ per hour were in the same range as in the sandstone, but at a higher level, between 100 and 150 ppm. The hydrogen concentration in the permeate chamber increased almost linearly during the first 42 h, before it declined in steepness. However, unlike in the sandstone experiment, no decrease in hydrogen concentration was measured throughout the entire experiment. The correction

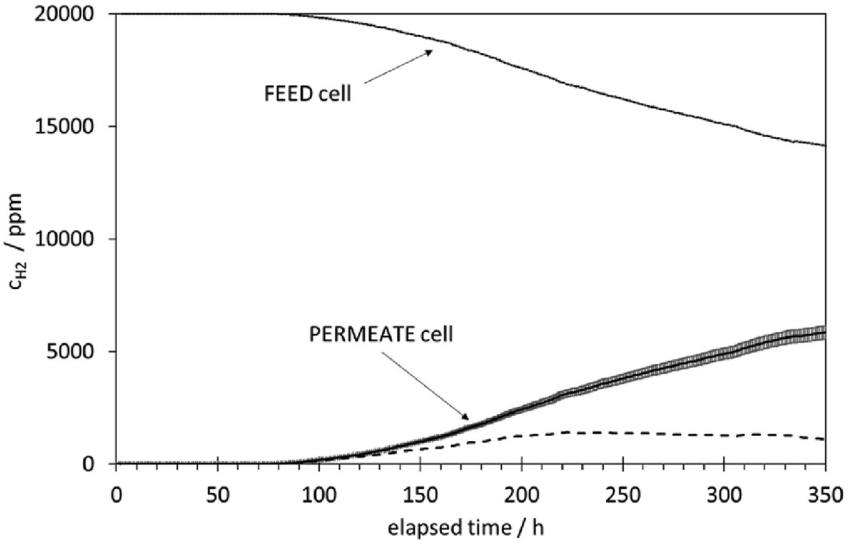

Fig. 5 – The diagram shows the course of the hydrogen concentration c_{H2} in the permeate and feed cell. Similar to the increase of hydrogen on the permeate side, the hydrogen concentration on the feed side decreased.

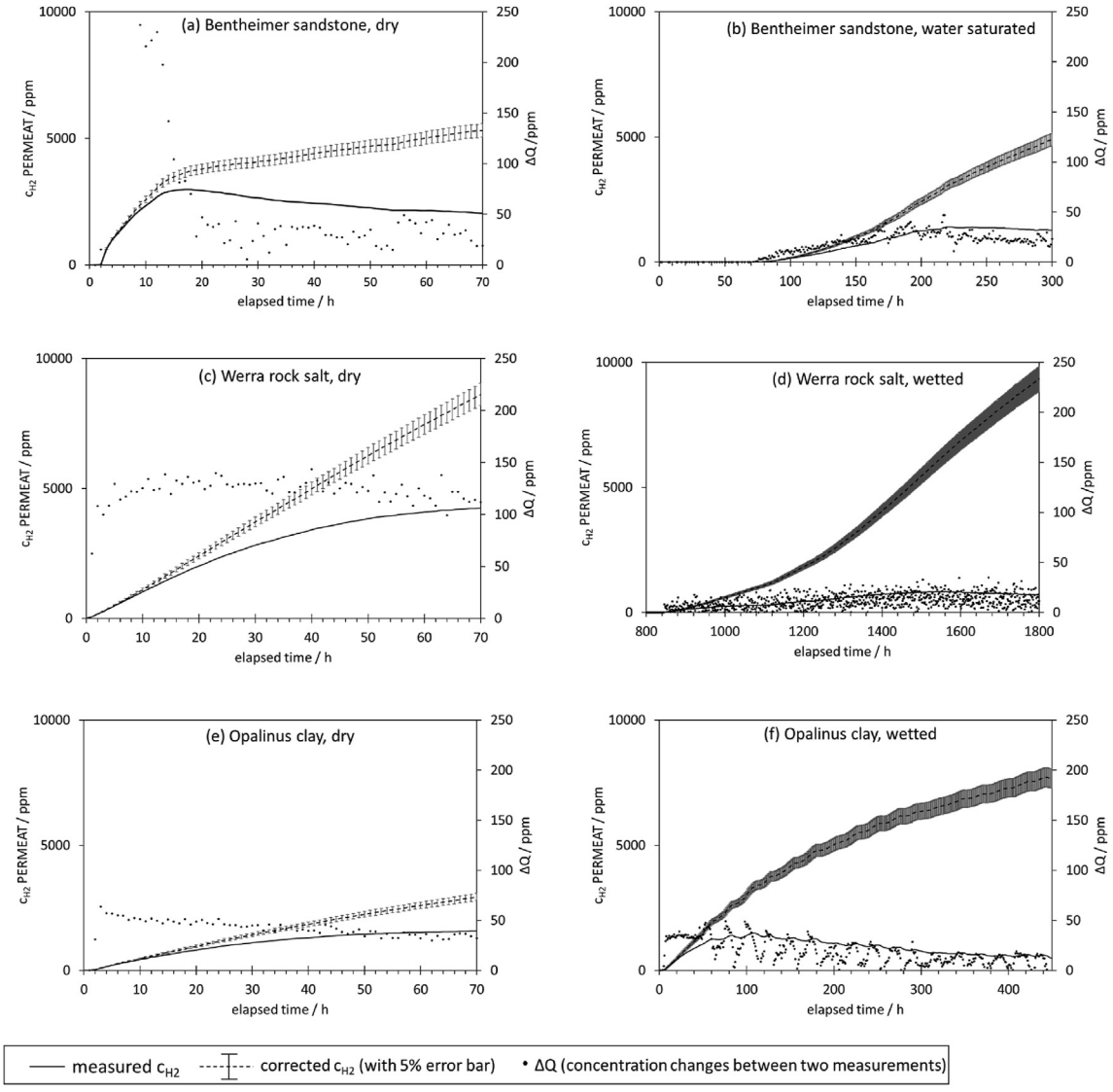

Fig. 6 – Diagrams showing the hydrogen concentration c_{H2} on the permeate side of diffusion experiments with dry and corresponding wet samples of Bentheimer sandstone, Werra rock salt and Opalinus clay. The solid black lines show the measured data, the dashed lines show corrected data with 5% error bars. The dots show the concentration differences between two adjacent measurements ΔQ and refer to the secondary y-axis. Diagrams on the left show dry rock experiments, on the right side, the results of the corresponding wet material are shown. Note, the time scale (x-axis) for the wetted samples on the righthand diagrams vary.

for hydrogen-loss shows a quasi linear trend of hydrogen increase in the permeate chamber. The equilibrium between the feed and the permeate chamber was established after 83 h. Data of the time range of 10–40 h were used to calculate the diffusion coefficient.

When similar experiments were carried out with Opalinus clay as a separator between the feed and permeate chamber, the hydrogen diffusion started similarly fast, between the first and second experimental hour. However, the hydrogen concentration on the feed side increased only slowly and the measured hydrogen concentrations barely exceeded 1500 ppm after 70 h of experimentation. The corrected hydrogen concentration on the permeate side reached about 3000 ppm after 70 h, which is much lower compared to Bentheimer sandstone and Werra rock salt. The concentration changes were about 70 ppm/h at the beginning of the experiment. They decreased continuously to finally 40 ppm/h. The scattering was much lower than in the experiments described above.

Measurements on wet sandstone, salt and clay material

In water-saturated Bentheimer sandstone, hydrogen exhibited a different diffusion behaviour (Fig. 6d). The breakthrough time of hydrogen was detected after more than 72 h. The detected hydrogen concentration on the permeate side did not exceed 1500 ppm and slowly decreased after a non-prominent maximum at 220 h elapsed time. The corrected values increased up to 3000 ppm in the same time interval and

continued to increase cumulatively until the experiment was terminated after 300 h. No equlilibrium between feed and permeate chamber was reached at this time. The concentration changes per hour ΔQ increased during the first 220 h to values up to 50 ppm/h, after that, ΔQ decreased to about 25 ppm/h. This is on concordance with the range of ΔQ for dry sandstone and suggests, that the pore-filling water was drained out of the sample, leaving the dry sandstone sample with interconnected pore spaces.

The wetted Werra rock salt plug was left untouched for one week to allow possible fractures to heal from the intruding and crystallizing brine percolating through the rock salt plug. The subsequent experiment indicate that previous migration pathways have reduced. Compared to the dry Werra rock salt equivalent, strong deviations were observed in terms of hydrogen breakthrough time and migration behaviour (Fig. 6d). The breakthrough time increased in the order of two magnitudes and was detected after 843 h. The concentration changes per hour (ΔQ) were considerably lower than in the dry rock experiment with values mainly below 25 ppm/h. Interestingly, the values were highly scattering, between 0 and 25 ppm/h, which persisted throughout the entire experimental duration. After about 1800 h, the experiment was finished and the equlibrium between hydrogen concentration in feed and permeate chamber (both chambers should contain 10,000 ppm of hydrogen) was almost reached.

The embedded Opalinus clay was carefully wetted on the surface facing the feed chamber and immediately placed in the diffusion cell. The resulting data show no noticeable changes between original and wetted clay material. Possibly, the effect of slight surface wetting is too small to cause changes in hydrogen diffusion. Most likely, the origninal sample was already humid and the additional wetting did not largely affect the sample. Interestingly, the hourly concentration changes ΔQ alternate with a frequency of about 24 h (Fig. 6f). That diurnal rhythm could be due the changes in room temperature by day/night shifts of room ventilation or air conditioning. The amplitude decreased in the course of the experiment, because of the decreasing hydrogen concentration gradient between feed and permeate chamber.

Hydrogen diffusion coefficients and breakthrough times of dry and wet sandstone, salt and clay material

Diffusion coefficients are important physical parameters of natural rocks. Large diffusion coefficients indicate that gas diffuses fast in the rocks [26]. Since only hydrogen was considered in the experiments, the gas properties (molecule size, geometric form) can be neglected here and the diffusion coefficient is only affected by the petrophysical rock properties, like porosity and permeability. Diffusion coefficients are not measured directly, but are calculated from the measured amount of gas diffusing through the rock in a given time using Fick's law.

The hydrogen diffusion coefficient is an indicator of the rate of hydrogen movement and suggestive for the gas transport mainly along micro fractures or through an interconnected pore space network. The hydrogen breakthrough times are additional indicators for rock tightness.

Breakthrough times of hydrogen for the investigated rock plugs vary between one and 843 h. The calculated hydrogen diffusion coefficients are in the region of 10^{-9} to 10^{-8} m^2/s. The flanking results were both generated in diffusion experiments for dry and wetted Werra rock salt. The lowest variations between data of dry and wet material were seen for the Opalinus clay. Here, both, hydrogen diffusion coefficient and breakthrough times were quite similar.

When wetted, the hydrogen diffusion rates decreased for all samples. That is mirrored by lower hydrogen diffusion coefficients and the increase in hydrogen breakthrough times (Fig. 7).

A hydrogen diffusion coefficient of 2.1×10^{-9} m^2/s was calculated for the dry Bentheimer sandstone plug. The difference of hydrogen diffusion coefficients between dry and

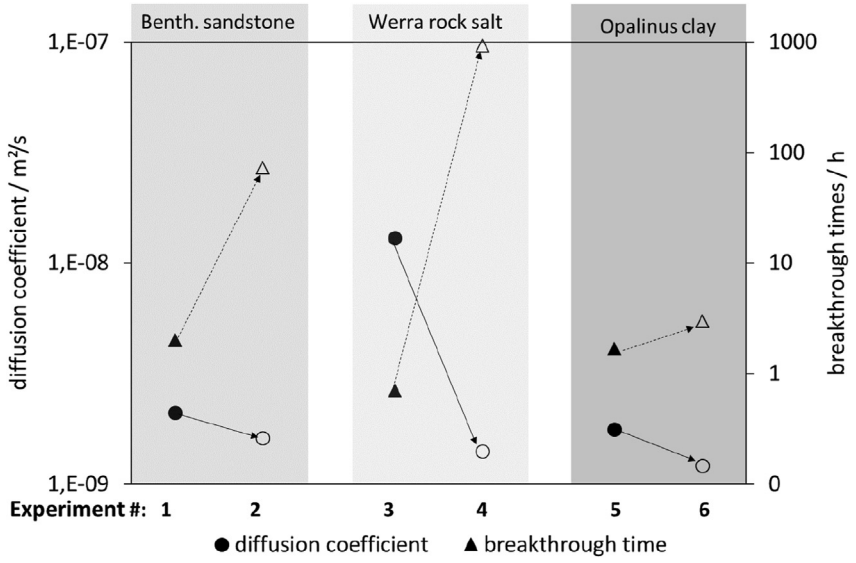

Fig. 7 – Diagram showing the diffusion coefficients and breakthrough times of the investigated Bentheimer sandstone, Werra rock salt and Opalinus clay samples. Closed symbols show dry material, open symbols show water-saturated and wetted samples. Arrows indicate changes of diffusion coefficients and breakthrough times in hydrogen through wet material.

wet Bentheimer sandstone was not prominent. The hydrogen diffusion coefficient of the water-saturated sandstone was calculated to be 1.6×10^{-9} m^2/s. More pronounced was the difference in hydrogen breakthrough times of a dry and water-saturated Bentheimer sandstone plugs. The data show, that the time for the hydrogen to reach the permeate chamber increased by more than an order of magnitude. While hydrogen breakthrough of the dry Bentheimer sandstone sample was detected after 2 h, the water-saturated Bentheimer sandstone sample retained hydrogen for 73 h. We assume, that at this time the water-filled pore space fell dry, probably due to the gravitational downward movement of the pore-filling liquid. The hydrogen diffusion coefficient is therefore only slightly reduced compared to the dry sample. As hydrogen diffusion coefficients in pure water range from 3.9 to 6.1×10^{-9} m^2/s [35–39], a somewhat lower diffusion coefficient, as determine here, is reasonable for a water-saturated sandstone, where, according to porosity data, 23.7% (pers. com. RWTH Aachen), pore space is now filled with water. The diffusion coefficient of the dry Bentheimer sandstone, however, seems to be too low. Assuming that the 23.7% of the sandstone sample consists of pore space is filled with air, hydrogen diffusion should occur faster, as the hydrogen diffusion coefficients in air are considerably higher, in the range from 0.756 to 1.604×10^{-4} m^2/s [39,41]. The reasons for the deviations from expectations might be, that the dry Bentheimer sandstone contains residual water in interparticle space) and the actually available migration pathway is smaller than assumed. Also, pore space might be not interconnected, so hydrogen diffusion through dry Bentheimer sandstone, where pores are filled with air, is considerable smaller than in pure air.

Hydrogen diffusion in saturated brine was stated by AbuAisha and Billiotte [40] with 4.6×10^{-9} m^2/s. An experiment using the Bentheimer sandstone, saturated with a brine of 200 g NaCl/L water, was conducted. It is not shown here, due to the absence of presentable data. In the course of the experiment, which was running for several month, no hydrogen breakthrough was detected and consequently, no diffusion coefficient could be determined. It is likely that the sandstone pores, and hence the preferential migration pathways, were clogged due to the precipitation of salt minerals in the pore space. As a result, a fairly hydrogen-tight sandstone plug evolved. Interestingly, the sample was even "hydrogen-tighter" than a wetted Werra rock salt sample.

Dry rock salt rarely comprises an open pore network for gas migration but micro fractures allow rapid movement of hydrogen. Experiment 3 (Table 1, Fig. 7) shows results of a Werra rock salt sample with a high diffusion coefficient of 1.3×10^{-8} m^2/s that strongly suggests micro fracturing. This is supported by the fast hydrogen breakthrough, within the first hour after the start of the experiment.

After wetting the surface of the Werra rock salt plug, the experiment was repeated. The hydrogen breakthrough time increased by three orders of magnitudes. The hydrogen diffusion coefficient also decreased noticeably, from 1.3×10^{-8} m^2/s to 1.4×10^{-9} m^2/s which indicates, that a widespread microcrack closure occurred by dissolution-recrystallisation processes. The hydrogen diffusion coefficient determined here, agrees with hydrogen diffusion coefficients of salt found in the literature, which are between 1×10^{-7} m^2/s and 6×10^{-12} m^2/s [43].

The experiments on fresh Opalinus clay (experiments 5 and 6 in Table 1 and Fig. 7) resulted in a hydrogen diffusion coefficient of 1.8×10^{-9} m^2/s. The sample was recovered during drilling at Mont Terri Rock Labor (BHS-1, drilling campaign in September 2021) and immediately packed and vacuumed in an aluminum foil bag. The diffusion experiments were performed in April 2022 and the sample was not preconditioned, e.g. dried, but used as it was. The additional, superficial wetting for experiment 6, caused no considerable decrease of the hydrogen diffusion coefficient. The hydrogen diffusion coefficient decreased only to 1.2×10^{-9} m^2/s. The hydrogen breakthrough time is about 2 h, which is in the same range as in experiment 5. Overall, the observed variations in breakthrough times and diffusion coefficients were small, which is likely because the difference between "dry" and "wetted" Opalinus clay is negligible. The term "dry" Opalinus clay is likely to be misleading, and only used in continuation to the previous samples of Bentheimer sandstone and Werra rock salt. In fact, the "dry" clay is in original conditions, and likely humid. Therefore, the difference between experiment 5 and 6 is small. In comparison to studies of Krooss [42] and Jacops [38], that state very low hydrogen diffusion coefficients of 3×10^{-11} m^2/s and 5.1×10^{-10} m^2/s, the results obtained here are considerably higher. We assume, that the differences are due to different measurement techniques. The study performed here, did neither apply water-saturated clayed samples, nor worked with dissolved hydrogen as diffusion agent.

This makes clear that extensive investigations are still necessary to determine reliable hydrogen diffusion coefficients.

Conclusion

The experimental set-up presented here, is suitable for the investigation of natural solid rock samples. Ideally, cores of 30 mm diameter are used. The length can vary. In the first experiments presented here, 10 mm thick plugs provided a well-manageable specimen size. Depending on rock characteristics, the sample length can be increased to at least 100 mm. Before the experiment, the plugs must be fixed in a through flange. This preparational work takes 3–5 days. The duration of the experiment depends on the material and its hydrogen breakthrough times, which can range from hours to month. Improvements should be considered in the sensor technique to avoid the application of correction equations.

We performed diffusion experiments with Bentheimer sandstone, Werra rock salt and Opalinus clay to obtain breakthrough times and calculate hydrogen diffusion coefficients for the respective rock sample. Overall, the observed hydrogen diffusion coefficients for whole-rock-samples are in the expected range between 10^{-9} to 10^{-8} m^2/s. In all experiments, water reduces the diffusion velocity. This is largely consistent with published data, e.g. 10^{-11} to 10^{-7} m^2/s for natural rocks [e.g. [43,57,58]]. Differences to published diffusion coefficients are due to different measurement methods, sample preparation and diffusion agent.

The hydrogen diffusion coefficients of dry and water-saturated Bentheimer sandstone were determined to be 2.1 and 1.6 $\times$ 10^{-9} m^2/s, respectively. The corresponding breakthrough times were 2 h and 73 h, respectively. A brine-saturated sample of Bentheimer sandstone appears to be impermeable to hydrogen within several month, possibly due to blockage of the pore space by intense salt mineralization throughout the entire sample plug.

The largest variations in breakthrough time and hydrogen diffusion coefficients were found for the Werra rock salt samples. While the dry sample has a diffusion coefficient of 1.3 $\times$ 10^{-8} m^2/s, the hydrogen diffusion coefficient of the wetted sample is, with 1.4 $\times$ 10^{-9} m^2/s, one order of magnitude lower. Furthermore, the fast breakthrough time of less than 1 h for the dry Werra rock salt has increased significantly. The wetted Werra rock salt shows the hydrogen breakthrough after 824 h. The cause for the strong differences is assumed to be fracture healing due to dissolution - precipitation effects within the Werra rock salt sample. The results are in the same order as literature reports. It is noteworthy, that the fully brine-saturated Bentheimer sandstone sample was even more impermeable to hydrogen. We assume, that the superficial wetting of the pure Werra rock salt had a smaller effect on fracture healing than the thorough brine-saturation of the Bentheimer sandstone sample, that caused an overall pore closure by salt precipitation.

The Opalinus clay in its original and wetted state does not show strong deviations, which is probably due to the fact, that the original sample was already moist. Overall, the determined hydrogen diffusion coefficients of 1.8 and 1.2 $\times$ 10^{-9} m^2/s, are higher than literature data. This is either due to differences in the analysis methodology or in the sample material. Preparation-related microcracks in the sample used cannot be completely ruled out either.

The results shown here, confirm the viability of the experimental set-up and provide a first approach to characterise and compare hydrogen gas transport through a variety of geological materials. The use of a correction equation allows for the compensation of hydrogen-losses or the use of a sensor with low hydrogen consumption. The set-up is therefore suitable as a "first-look-method" or for comparing different consolidated rock types to obtain data on hydrogen diffusion coefficients and breakthrough times. Following the rather unspecific approach applied here in terms of water saturation or dryness of rock samples, a thorough study is needed to quantify the effects of gaseous and liquid pore filling and the effects of salt precipitation from brine.

Declaration of competing interest

The authors declare that they have no known competing financial interests or personal relationships that could have appeared to influence the work reported in this paper.

Acknowledgement

This study was part of the project H2React2 and we gratefully acknowledge the financial support of the BMBF under grant no. 03G0902B.

REFERENCES

[1] Aslannezhad M, Ali M, Kalantariasl A, Sayyafzadeh M, You Z, Iglauer S, Keshavarz A. A review of hydrogen/rock/brine interaction: implications for Hydrogen Geo-storage. Prog Energy Combust Sci 2023;95. https://doi.org/10.1016/j.pecs.2022.101066.

[2] Dawood F. Hydrogen production for energy: an overview. Int J Hydrogen Energy 2020;45:3847–69. https://doi.org/10.1016/j.ijhydene.2019.12.059.

[3] Yue M, Lambert H, Pahon E, Roche R, Jemei S, Hissel D. Hydrogen energy systems: a critical review of technologies, applications, trends and challenges. Renew Sustain Energy Rev 2021;146:111180. https://doi.org/10.1016/j.rser.2021.111180.

[4] Com EP. Communication from the commission to the European parliament, the council, the European economic and social committee and the committee of the regions. A hydrogen strategy for a climate-neutral europe. 2020. European Commission, COM/2020/301 final, https://eur-lex.europa.eu/legal-content/EN/TXT/?uri=CELEX:52020DC0301.

[5] NWS. Bundesministerium für Wirtschaft und Energie: die Nationale Wasserstoffstrategie. 2020. https://www.bmwi.de/Redaktion/DE/Publikationen/Energie/die-nationale-wasserstoffstrategie.html.

[6] Zivar D, Kumar S, Foroozesh J. Underground hydrogen storage: a comprehensive review. Int J Hydrogen Energy 2020;46(Issue 45):23436–62. https://doi.org/10.1016/j.ijhydene.2020.08.138.

[7] Sterner M, Stadler I, editors. Handbook of energy storage - demand, technologies, integration. Springer-Verlag Berlin - Heidelberg; 2019. p. 748. ISBN978-3-662-55503-3.

[8] Pudlo D, Ganzer L, Henkel S, Kühn M, Liebscher A, De Lucia M, Panfilov M, Pilz P, Reitenbach V, Albrecht D, Würdemann H, Gaupp R. The H2STORE project: hydrogen underground storage - a feasible way in storing electrical power in geological media? Clean energy systems in the subsurface: production, storage and conversion, vols. 395–412. Springer Berlin; 2013. https://doi.org/10.1007/978-3-642-37849-2_31.

[9] Warnecke M, Röhling S. Untertägige speicherung von Wasserstoff - status quo. Z Dtsch Ges Geowiss 2021. https://doi.org/10.1127/zdgg/2021/0295. Open Access Article.

[10] Amid A, Mignard D, Wilkinson M. Seasonal storage of hydrogen in a depleted natural gas reservoir. Int J Hydrogen Energy 2016;41(Issue 12):5549–58. https://doi.org/10.1016/j.ijhydene.2016.02.036.

[11] Epelle EI, Obande W, Udourioh GA, Afolabi IC, Desongu KS, Orivri U, Gunes B, Okolie JA. Perspectives and prospects of underground hydrogen storage and natural hydrogen. Sustain Energy Fuels 2022;6:3324–43. https://doi.org/10.1039/D2SE00618A.

[12] Liebscher A, Wackerl J, Streibel M. Geologic storage of hydrogen - fundamentals, processing, and projects. In: Hydrogen science and engineering : materials, processes, systems and technology; 2016. https://doi.org/10.1002/9783527674268.ch26.

[13] Rudolph T. Underground hydrogen storage - current developments and opportunities. EAGE/DGMK Joint Workshop on Underground Storage of Hydrogen 2019. https://doi.org/10.3997/2214-4609.201900256.

[14] Sáinz-García A, Abarca E, Rubí V, Grandia F. Assessment of feasible strategies for seasonal underground hydrogen storage in a saline aquifer. Int J Hydrogen Energy 2017:16657–66. https://doi.org/10.1016/j.ijhydene.2017.05.076. 42.

[15] Seliger U, Wegner S, Voigt-Jungton J. Untersuchung der Diffusion von Kohlenmonoxid durch Baustoffe. Forschungsbericht Nr 2019;195. Hayrothsberge, FA Nr. 94 (2/2017) IdF ISSN 170-0060.
[16] Shi Z, Jessen K, Tsotsis TT. Impacts of the subsurface storage of natural gas and hydrogen mixtures. Int J Hydrogen Energy 2020;45(Issue 15):8757–73. https://doi.org/10.1016/j.ijhydene.2020.01.044.
[17] Ali M, Yekeen N, Pal N, Keshavarz A, Iglauer S, Hoteit H. Influence of pressure, temperature and organic surface concentration on hydrogen wettability of caprock; implications for hydrogen geo-storage. Energy Rep 2021;7:5988–96. https://doi.org/10.1016/j.egyr.2021.09.016.
[18] Esfandyari H, Hosseini M, Ali M, Iglauer S, Haghighi M, Keshavarz A. Assessment of the interfacial properties of various mineral/hydrogen/water systems. J Energy Storage 2023;52. https://doi.org/10.1016/j.est.2022.104866. Part A.
[19] Hosseini M, Fahimpour J, Ali M, Keshavarz A, Iglauer S. Hydrogen wettability of carbonate formations: implications for hydrogen geo-storage. J Colloid Interface Sci 2022;614:256–66. https://doi.org/10.1016/j.jcis.2022.01.068.
[20] Iglauer S, Ali M, Keshavarz A. Hydrogen wettability of sandstone reservoirs: implications for hydrogen geo-storage. Geophys Res Lett 2021;48:e2020GL090814. https://doi.org/10.1029/2020GL090814.
[21] Keshavarz A, Abid H, Ali M, Iglauer S. Hydrogen diffusion in coal: implications for hydrogen geo-storage. J Colloid Interface Sci 2022;608(2):1457–62. https://doi.org/10.1016/j.jcis.2021.10.050.
[22] Anikeev DP, Zakirov ES, Indrupskiy IM, Anikeeva ES. Estimation of diffusion losses of hydrogen during the creation of its effective storage in an aquifer. SPE Russian Petroleum Technology Conference 2021. https://doi.org/10.2118/206614-MS. SPE-206614-MS.
[23] De Lucia M, Pilz P, Liebscher A, Kühn M. Measurements of H_2 solubility in saline solutions under reservoir conditions: preliminary results from project H2STORE. Energy Proc 2015;76:487–94. https://doi.org/10.1016/j.egypro.2015.07.892.
[24] Hagemann B, Panfilov M, Ganzer L. Multicomponent gas rising through water with dissolution in stratified porous reservoirs – application to underground storage of H_2 and CO_2. J Nat Gas Sci Eng 2016;31:198–213. https://doi.org/10.1016/j.jngse.2016.03.019.
[25] Hassanpouryouzband A, Adie K, Cowen T, Thaysen EM, Heinemann N, Butler IB, Wilkinson M, Edlmann K. Geological hydrogen storage: geochemical reactivity of hydrogen with sandstone reservoirs. ACS Energy Lett 2022;7:2203–10. https://doi.org/10.1021/acsenergylett.2c01024. 2022.
[26] Guangdi L, Zhongying Z, Mingliang S, Jian L, Guoyi H, Xiaobo W. New insights into natural gas diffusion coefficient in rocks. Petrol Explor Dev 2012;39(5):597–604. https://doi.org/10.1016/S1876-3804(12)60081-0.
[27] Krooss BM, Leythaeuser D. Experimental measurements of the diffusion parameter of light hydrocarbons in water-saturated sedimentary rocks - II. Results and geochemical significance. Org Geochem 1987;12(2):91–108. https://doi:10.1016/0146-6380(88)90247-1.
[28] Peng S, Hu Q, Hamamoto S. Diffusivity of rocks: gas diffusion measurements and correlation to porosity and pore size distribution. Water Resources Reserch 2012;48:W02507. https://doi.org/10.1029/2011WR011098.
[29] Graham T. On the absorption and dialytic separation of gases by colloid septa. Philosophical transactions of the Royal Society of London 1866;156(Nr.):399–439.
[30] Smithells CJ, Ransley CE. The diffusion of gases through metals, vol. 150. Proceedings of the royal Soc. A publishing; 1935. p. 869. https://doi.org/10.1098/rspa.1935.0095.
[31] Stross TM, Tompkins FC. The diffusion coefficient of hydrogen in iron. J Chem Soc 1956:230–4. https://doi.org/10.1039/JR9560000230.
[32] Johnson EW. The diffusivity of hydrogen in alpha iron. Transactions of the Metallurgical Society of AIME 1960;218(12):1104–12.
[33] Oriani RA. The diffusion and trapping of hydrogen in steel. Acta Metall 1970;18:147–57. https://doi.org/10.1016/0001-6160(70)90078-7.
[34] Addach H, Bercot P, Rezrazi M, Wery M. Hydrogen Permeation in iron at different temperatures. Mater Lett 2005;59:1347–51. https://doi.org/10.1016/j.matlet.2004.12.037.
[35] Blok WJ, Fortuin J, Vermeulen DP. Bestimmung des Diffusionskoeffizienten von Wasserstoff in Wasser und wässerigen Polymerlösungen nach der CBS-Methode. Wärme und Stoffübertragung 1982;17:11–6. https://doi.org/10.1007/BF01686960.
[36] Ferrell RT, Himmelblau DM. Diffusion coefficients of hydrogen and helium in water. AIChE J 1967;13:702–8. https://doi.org/10.1002/aic.690130421.
[37] Hemme C, van Berk W. Hydrogeochemical modeling to identify potential risks of underground hydrogen storage in depleted gas fields. Appl Sci 2018. https://doi.org/10.3390/APP8112282.
[38] Jacops E, Aertsens M, Maes N, Bruggeman C, Krooss BM, Amann-Hildenbrand A, Swennen R, Littke R. Interplay of molecular size and pore network geometry on the diffusion of dissolved gases and HTO in Boom Clay. Appl Geochem 2017;76:182–95. https://doi.org/10.1016/j.apgeochem.2016.11.022.
[39] Mostinsky IL. Diffusion coefficient. Thermopedia; 2011. https://doi.org/10.1615/AtoZ.d.diffusion_coefficient.
[40] AbuAisha MS, Billiotte J. A discussion on hydrogen migration in rock salt for tight underground storage with an insight into a laboratory setup. J Energy Storage 2021;38. https://doi.org/10.1016/j.est.2021.102589.
[41] Engineering ToolBox. Air - Diffusion Coefficients of Gases in Excess of Air 2018 [online] Available at: https://www.engineeringtoolbox.com/air-diffusion-coefficient-gas-mixture-temperature-d_2010.html. [Accessed 6 February 2023].
[42] Krooss B. Evaluation of database on gas migration through clayey host rocks. Belgian National Agency for Radioactive Waste and Enriched Fissile. Material (ONDRAF-NIRAS) 2008.
[43] Müller-Lyda I. Erzeugung und Verbleib von Gasen in einem Endlager für radioaktive Abfälle. Bericht über den GRS-Workshop vom 29. und 30. Mai 1996 in Braunschweig, Gesellschaft für Anlagen und Reaktorsicherheit, vol. 129. GRS) mbH GRS -; 1997, ISBN 3-923875-89-4.
[44] Wiegleb G. Gasmesstechnik in Theorie und Praxis. Wiesbaden: Springer Vieweg Verlag; 2016, ISBN 978-3-658-10687-4.
[45] Peksa AE, Karl-Heinz AA, Pacelli W, Zitha LJ. Bentheimer sandstone revisited for experimental purposes. Mar Petrol Geol 2015;67:701–19. https://doi.org/10.1016/j.marpetgeo.2015.06.001. ISSN 0264-8172.
[46] Dubelaar W, Nijland CTG. The bentheim sandstone: geology, petrophysics, varieties and its use as dimension stone. In: Lollino G, Giordan D, Marunteanu C, Christaras B, Yoshinori I, Margottini C, editors. Engineering geology for society and territory, vol. 8. Cham: Springer; 2015. https://doi.org/10.1007/978-3-319-09408-3_100.

[47] Strauch B, Richter H, Zimmer M, Giese R, Zirkler A. Underground in-situ investigation of spatial and temporal changes of rock salt integrity in the marginal area of a natural CO2-rich cavernous structure. Appl Geochem 2022;139:105264. https://doi.org/10.1016/j.apgeochem.2022.105264.
[48] Stormont JC. Gas permeability changes in rock salt during deformation. Ph.D. Thesis. Tucson, AZ: University of Arizona; 1990.
[49] Al Reda SM, Yu C, Berthe G, Matray J-M. Study of the permeability in the Opalinus clay series (Mont Terri - Switzerland) using the steady state method in Hassler cell. J Petrol Sci Eng 2020;184:106457. https://doi.org/10.1016/j.petrol.2019.106457. ISSN 0920-4105.
[50] Bock H. RA Experiment. Rock mechanics analyses and synthesis: data report on rock mechanics. Mont Terri Project; 2001. Technical Report 2000-02.
[51] Jacops E, Grade A, Govaerts J, Maes N. Measuring the diffusion coefficient of He in opalinus clay. SCK-CEN ER-238. Mol, Belgium: SCK†CEN; 2013.
[52] Strauch B, Pilz P, Zimmer M, Kujawa C. Results of experimental simulations on hydrogen migration through potential storage rocks. GFZ Data Services; 2023. https://doi.org/10.5880/GFZ.3.1.2023.001.
[53] Strauch B, Pilz P, Hierold J, Zimmer M. Abstracts, GeoKarlsruhe 2021. In: Experimental simulations of hydrogen migration through potential storage rocks; 2021. Online, Karlsruhe, Germany 2021), https://gfzpublic.gfz-potsdam.de/pubman/item/item_5009080.
[54] Krooss BM, Schaefer RG. Experimental measurements of the diffusion parameters of light hydrocarbons in water-saturated sedimentary rocks - I. A new experimental procedure. Org Geochem 1986;11:193–9. https://doi.org/10.1016/0146-6380(87)90022-2.
[55] Yaroshchuk AE, Glaus MA, Van Loon LR. Diffusion through confined media at variable concentrations in reservoirs. J Membr Sci 2008;319:133–40. https://doi.org/10.1016/j.memsci.2008.03.027.
[56] Geiker M, Grube H, Luping T, Nielsson LO, Andrade C. Laboratory test methods. In: Kropp J., Hilsdorf H.K. (editors). RILEM Report 12. Performance criteria for concrete durability; ISBN 0-203-63053-X,1995.
[57] Jacops E, Wouters K, Volckaert G, Moors H, Maes N, Bruggeman C, Swennen R, Littke R. Measuring the effective diffusion coefficient of dissolved hydrogen in saturated Boom Clay. Measuring the effective diffusion coefficient of dissolved hydrogen in saturated Boom Clay. Appl Geochem 2015;61(175–184). https://doi.org/10.1016/j.apgeochem.2015.05.022. ISSN 0883-2927.
[58] Pfeiffer WT, Beyer C, Bauer S. Hydrogen storage in a heterogeneous sandstone formation: dimensioning and induced hydraulic effects. Petrol Geosci 2017;23(3):315. https://doi.org/10.1144/petgeo2016-050.